

The trouble with H_0

José Luis Bernal^{a,b} Licia Verde^{a,c,d,e,f} Adam G. Riess^{g,h}

^aICC, University of Barcelona, IEEC-UB, Martí i Franquès, 1, E08028 Barcelona, Spain

^bDept. de Física Quàntica i Astrofísica, Universitat de Barcelona, Martí i Franquès 1, E08028 Barcelona, Spain

^cICREA, Pg. Llus Companys 23, 08010 Barcelona, Spain

^dRadcliffe Institute for Advanced Study, Harvard University, MA 02138, USA

^eInstitute of Theoretical Astrophysics, University of Oslo, 0315, Oslo, Norway

^fInstitute for Theory and Computation, Harvard-Smithsonian Center for Astrophysics, 60 Garden Street, Cambridge, MA 02138, USA

^gDepartment of Physics and Astronomy, Johns Hopkins University, Baltimore, MD 21218

^hSpace Telescope Science Institute, 3700 San Martin Drive, Baltimore, MD 21218

E-mail: joseluis.bernal@icc.ub.edu, ariess@stsci.edu, liciaverde@icc.ub.edu

Abstract. We perform a comprehensive cosmological study of the H_0 tension between the direct local measurement and the model-dependent value inferred from the Cosmic Microwave Background. With the recent measurement of H_0 this tension has raised to more than 3σ . We consider changes in the early time physics without modifying the late time cosmology. We also reconstruct the late time expansion history in a model independent way with minimal assumptions using distances measures from Baryon Acoustic Oscillations and Type Ia Supernovae, finding that at $z < 0.6$ the recovered shape of the expansion history is less than 5% different than that of a standard Λ CDM model. These probes also provide a model insensitive constraint on the low-redshift standard ruler, measuring directly the combination $r_s h$ where $H_0 = h \times 100$ km/s/Mpc and r_s is the sound horizon at radiation drag (the standard ruler), traditionally constrained by CMB observations. Thus r_s and H_0 provide absolute scales for distance measurements (anchors) at opposite ends of the observable Universe. We calibrate the cosmic distance ladder and obtain a model-independent determination of the standard ruler for acoustic scale, r_s . The tension in H_0 reflects a mismatch between our determination of r_s and its standard, CMB-inferred value. Without including high- ℓ Planck CMB polarization data (i.e., only considering the “recommended baseline” low- ℓ polarisation and temperature and the high ℓ temperature data), a modification of the early-time physics to include a component of dark radiation with an effective number of species around 0.4 would reconcile the CMB-inferred constraints, and the local H_0 and standard ruler determinations. The inclusion of the “preliminary” high- ℓ Planck CMB polarisation data disfavours this solution.

Contents

1	Introduction	1
2	Data	3
3	Methods	5
4	Modifying early Universe physics: effect on H_0 and r_s	6
4.1	Changing the details of recombination: $Y_{\text{p}}^{\text{BBN}}$	6
4.2	Changing early time expansion history: ΔN_{eff}	7
5	Changing late-time cosmology	9
5.1	Reconstruction independent from the early-time physics	13
5.2	Reconstruction with free curvature	16
6	Discussion and Conclusions	17

1 Introduction

In the last few years, the determination of cosmological parameters has reached astonishing and unprecedented precision. Within the standard Λ - Cold Dark Matter (Λ CDM), cosmological model some parameters are constrained at or below the percent level. This model assumes a spatially flat cosmology and matter content dominated by cold dark matter but with total matter energy density dominated by a cosmological constant, which drives a late time accelerated expansion. Such precision has been driven by a major observational effort. This is especially true in the case of Cosmic Microwave Background (CMB) experiments, where WMAP [1, 2] and Planck [3] have played a key role, but also in the measurements of Baryon Acoustic Oscillations (BAO) [4, 5], where the evolution of the cosmic distance scale is now measured with a $\sim 1\%$ uncertainty.

The Planck Collaboration 2015 [3] presents the strongest constraints so far in key parameters, such as geometry, the predicted Hubble constant, H_0 , and the sound horizon at drag epoch, r_s . These last two quantities provide an absolute scale for distance measurements at opposite ends of the observable Universe (see e.g., [6, 7]), which makes them essential to build the distance ladder and model the expansion history of the Universe. However, they are *indirect* measurements and as such they are model-dependent. Whereas the H_0 constraint assumes an expansion history model (which heavily relies on late time physics assumptions such as the details of late-time cosmic acceleration, or equivalently, the properties of dark energy), r_s is a derived parameter which relies on early time physics (such as the density and equation of state parameters of the different species in the early universe).

This is why having model-independent, direct measurements of these same quantities is of utmost importance. In the absence of significant systematic errors, if the standard cosmological model is the correct model, indirect (model-dependent) and direct (model-independent) constraints on these parameters should agree. If they are significantly inconsistent, this will provide evidence of physics beyond the standard model (or unaccounted systematic errors).

Direct measurements of H_0 rely on the ability to measure absolute distances to > 100 Mpc, usually through the use of coincident geometric and relative distance indicators. H_0 can be interpreted as the normalization of the Hubble parameter, $H(z)$, which describes the expansion rate of the Universe as function of redshift. Previous constraints on H_0 (i.e. [8]) are consistent with the final results from the WMAP mission, but are in $2\text{--}2.5\sigma$ tensions with Planck [9–11]. The low value of H_0 found, within the Λ CDM model, by the Planck Collaboration since its first data release [12], and confirmed by the latest data release [3], has attracted a lot of attention. Re-analyses of the direct measurements of H_0 have been performed ([13] including the recalibration of distances of [14]); physics beyond the

standard model has been advocated to alleviate the tension, especially higher number of effective relativistic species, dynamical dark energy and non-zero curvature [15–19].

In some of these model extensions, by allowing the extra parameter to vary, tension is reduced but this is mainly due to weaker constraints on H_0 (because of the increased number of model parameters), rather than an actual shift in the central value. In many cases, non-standard values of the extra parameter appear disfavoured by other data sets.

Recent improvements in the process of measuring H_0 (an increase in the number of SNeIa calibrated by Cepheids from 8 to 19, new parallax measurements, stronger constraints on the Hubble flow and a refined computation of distance to NGC4258 from maser data) have made possible a 2.4% measurement of H_0 : $H_0 = 73.24 \pm 1.74$ km/s/Mpc [20]. This new measurement increases the tension with respect to the Planck-inferred value to $\sim 3.4\sigma$.

Time-delay cosmography measurements of quasars which pass through strong lenses is another way to set independent constraints on H_0 . Effort in this direction is represented by the H0LiCOW project [21]. Using three strong lenses, they find $H_0 = 71.9^{+2.4}_{-3.0}$ km/s/Mpc, within flat Λ CDM with free matter and energy density [22]. Fixing $\Omega_M = 0.32$ (motivated by the Planck results [3]), yields a value $H_0 = 72.8 \pm 2.4$ km/s/Mpc. These results are in 1.7σ and 2.5σ tension with respect to the most-recent CMB inferred value, while are perfectly consistent with the local measurement of [20].

In addition, in [23], it is shown that the value of H_0 depends strongly on the CMB multipole range analysed. Analysing only temperature power spectrum, tension of 2.3σ between the H_0 from $\ell < 1000$ and from $\ell \geq 1000$ is found, the former being consistent with the direct measurement of [20].

All this could be interpreted as a hint of internal inconsistencies in Planck data or of physics beyond the standard model. These recent results clearly motivate a detailed study of possible extensions of the Λ CDM model and an inspection of the current cosmological data sets, checking for inconsistencies.

In figure 1, we summarize the current constraints on H_0 tied to the CMB and low-redshift measurements. We show results from the public posterior samples provided by the Planck Collaboration 2015 [3], WMAP9 [1] (analysed with the same assumptions of Planck)¹, the results of the work of Addison et al. [23] and the quasar time-delay cosmography measurements of H_0 [22], along with the local measurement of [20]. CMB constraints are shown for two models: a standard flat Λ CDM and a model where the effective number of neutrino species N_{eff} is varied in addition to the standard Λ CDM parameters. Of all the popular Λ CDM model extensions, this is the most promising one to reduce the tension.

On the other hand, r_s is the standard ruler which calibrates the distance scale measurements of BAO. However, since BAO measure D_V/r_s (or D_A/r_s and Hr_s in the anisotropic analysis) the only way to constrain r_s without making assumptions about the early universe physics is combining the BAO measurement with other probes of the expansion rate (such as H_0 , cosmic clocks [26] or gravitational lensing time delays [21]). This was illustrated in [27] and more recently in [28], where only weak assumptions are made on the shape of $H(z)$, and in [6], where the normal and inverse distance ladder are studied in the context of Λ CDM and typical extensions.

When no cosmological model is assumed, H_0 and r_s are understood as anchors of the cosmic distance ladder and the inverse cosmic distance ladder, respectively. If the universe expansion history is probed by observations such as BAO and SNeIa, the two anchors are related by $H_0 r_s = \text{constant}$.

While the model-independent measurement of r_s [27] is consistent with Planck, the model-dependent value of [6] is in 2σ tension with it. Both of these measurements use $H_0 = 73.0 \pm 2.4$, so, this modest tension is expected to increase with the new constraint on H_0 which leaves the central value almost unchanged but has significantly smaller error-bars.

In this paper we quantify the tension in H_0 and explore how it could be resolved –without invoking systematic errors in the measurements– by studying separately changes in the early time physics and in the late time physics

¹The values of r_s in WMAP’s public posterior samples were computed using the approximation of [24], which is inaccurate by several percent, as pointed in the appendix B of Ref. [25]. As WMAP’s data have been re-analysed by the Planck Collaboration, the values reported here are computed correctly.

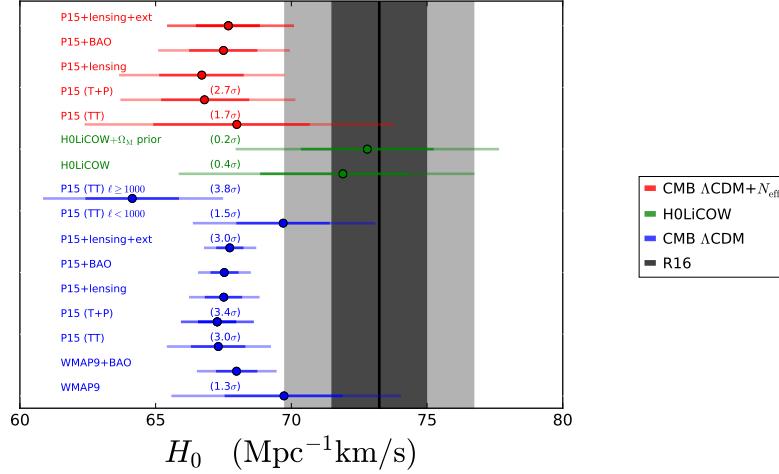


Figure 1. Marginalised 68% and 95% constraints on H_0 from different analysis of CMB data, obtained from Planck Collaboration 2015 public chains [3], WMAP9 [1] (analysed with the same assumptions than Planck) and the results of the work of Addison et al. [23] and Bonvin et al. [22]. We show the constraints obtained in a Λ CDM context in blue, Λ CDM+ N_{eff} in red, quasar time-delay cosmography results (taken from H0LiCOW project [22], for a Λ CDM model, with and without relying on a CMB prior for Ω_M) in green and the constraints of the independent direct measurement of [20] in black. We report in parenthesis the tension with respect to the direct measurement in the cases of interest. Note that WMAP9+BAO uses BAO measurement with Planck values of the sound horizon, and that is why the central values are so different.

We follow three avenues. Firstly, we allow the early cosmology (probed mostly by the CMB) to deviate from the standard Λ CDM assumptions, leaving unaltered the late cosmology (e.g., the expansion history at redshift below $z \sim 1000$ is given by the Λ CDM model). Secondly, we allow for changes in the late time cosmology, in particular in the expansion history at $z \leq 1.3$, assuming standard early cosmology (i.e., physics is standard until recombination, but the expansion history at late time is allowed to be non-standard). Finally, we reconstruct in a model-independent way, the late-time expansion history without making any assumption about the early-time physics, besides assuming that the BAO scale corresponds to a standard ruler (with unknown length). By combining BAO with SNeIa and H_0 measurements we are able to measure the standard ruler in a model-independent way. Comparison with the Planck-derived determination of the sound horizon at radiation drag allows us to assess the consistency of the two measurements within the assumed cosmological model.

In section 2 we present the data sets used in this work and in section 3 we describe the methodology. We explore modifications of early-time physics from the standard Λ CDM (leaving unaltered the late-time ones) in section 4 while changes in the late-time cosmology are explored in section 5. Here we present the findings both assuming standard early-time physics and in a way that is independent from it. Finally we summarize the conclusions of this work in section 6.

2 Data

The observational data we consider are: measurements of the Cosmic Microwave Background (CMB), Baryon Acoustic Oscillations (BAO), Type Ia Supernovae (SNeIa) and direct measurements of the Hubble constant H_0 .

We consider the full Planck 2015 temperature (TT), polarization (EE) and the cross correlation of temperature and polarization (TE) angular power spectra, (C_ℓ) [3], corresponding to the following likelihoods: *Planck* high ℓ ($30 \leq \ell \leq 2508$) TTTEEE for TT (high ℓ TT), EE and TE (high ℓ TEEE) and the *Planck* low ℓ for TT, EE, TE and BB (lowTEB, $2 \leq \ell \leq 29$). The Planck team [3, 29] identifies the lowTEB + high ℓ TT as the “recommended baseline” dataset and the high ℓ polarisation (high ℓ

Survey	z_{eff}	Parameter	Measurement
6dF [30]	0.106	r_s/D_V	0.327 ± 0.015
SDSS-MGS [31]	0.15	D_V/r_s	4.47 ± 0.16
BOSS-LOWZ [5]	0.32	D_V/r_s	8.59 ± 0.15
WiggleZ [32]	0.44	D_V/r_s	11.6 ± 0.6
BOSS-CMASS [5]	0.57	D_V/r_s	13.79 ± 0.14
BOSS-CMASS [5]	0.57	D_A/r_s	9.52 ± 0.14
BOSS-CMASS [5]	0.57	Hr_s	14750 ± 540
WiggleZ [32]	0.6	D_V/r_s	15.0 ± 0.7
WiggleZ [32]	0.73	D_V/r_s	16.9 ± 0.6

Table 1. BAO data measurements included in our analysis changing the early cosmology specifying the survey that obtained each measurement and the corresponding effective redshift z_{eff} . In the case where we change the late time cosmology, we use the isotropic measurements. We take into account the correlation between the anisotropic measurements of BOSS-CMASS and among the values from WiggleZ.

TEEE) as “preliminary”, because of evidence of low level systematics ($\sim (\mu K)^2$ in $\ell(\ell+1)C_\ell$). While the level of systematic contamination does not appear to affect parameter estimation, we nevertheless present result both excluding and including the high ℓ polarisation data. In addition, we use the lensing reconstruction signal for the range $40 \leq L \leq 400$. We distinguish between the CMB power spectra and the lensing reconstruction by referring to the latter as CMB lensing. For some models we use the publicly available posterior samples (i.e., public chains) provided by the Planck collaboration: Λ CDM, Λ CDM+ N_{eff} (a base Λ CDM model with an extra parameter for the effective number of neutrino species) and Λ CDM+ Y_P (a base Λ CDM model with an extra parameter for the primordial Helium abundance). In addition, we use the analysis of WMAP9 data with the same assumptions of Planck, which is publicly available along with the rest of Planck data. We also use the results of Addison et al. [23], where the Planck’s temperature power spectrum is analysed in two separate multipole ranges: $\ell < 1000$ and $\ell \geq 1000$.

We use constraints on BAO from the following galaxy surveys: Six Degree Field Galaxy Survey (6dF) [30], the Main Galaxy Sample of Data Release 7 of Sloan Digital Sky Survey (SDSS-MGS) [31], the LOWZ and CMASS galaxy samples of the Baryon Oscillation Spectroscopic Survey (BOSS-LOWZ and BOSS-CMASS, respectively) [5], and the reanalysed measurements of WiggleZ [32]. These measurements, and their corresponding effective redshift z_{eff} , are summarized in table 1. Note that for BOSS-CMASS there is an isotropic measurement (D_V/r_s) and an anisotropic measurement (D_A/r_s , Hr_s), which, of course, we never combine. The anisotropic measurement is used in section 4.2. When we use the anisotropic values from BOSS-CMASS, we take into account that they are correlated. In the case where we change the late time physics, we use always the isotropic measurements of BAO with a sound horizon coming from an analysis of the CMB independent of late Universe physics (r_s^{early} from [33]), as specified in section 5. In both cases, we use the covariance matrix for the measurements of WiggleZ as indicated in Ref. [32]. We consider that the measurements of BOSS-CMASS and WiggleZ are independent, although the regions covered by both surveys overlap. We can do so because this overlap includes a small fraction of the BOSS-CMASS sample and the correlation is very small too (always below 4%) [5, 34], hence the constraints which come from both surveys are fairly independent. The BOSS collaboration also provides a BAO measurement at $z \sim 2.5$ obtained from Lyman α forest observed in Quasars spectra. We do not include this measurement because, as it will be clear later, our approach relies on having BAO and SNeIa data covering roughly the same redshift range. Considering an extra BAO point at high redshift would have increased the number of parameters needed to describe the expansion history without improving constraints in any of the quantities we are interested in.

The publicly available Planck 2015 posterior sampling uses a slightly different BAO data set (see Ref. [3] for details). However the small difference in the data set does not drive any significant effect in the parameter constraints.

For SNeIa cosmological observations, we use the SDSS-II/SNLS3 Joint Light-curve Analysis (JLA) data compilation [35]. This catalog contains 740 spectroscopically confirmed SNeIa obtained from low redshift samples ($z < 0.1$), all three seasons of the Sky Digital Sky Survey II (SDSS-II) ($0.05 < z < 0.4$) and the three years of the SuperNovae Legacy Survey (SNLS) ($0.2 < z < 1$) together with nine additional SNeIa at high redshift from HST ($0.8 < z < 1.3$). We use the compressed form of the JLA likelihood (Appendix E of Ref. [35]).

Finally, we use the distance recalibrated direct measurement of H_0 from [20], which is $H_0 = 73.24 \pm 1.74 \text{ Mpc}^{-1}\text{km/s}$.

3 Methods

We use the public Boltzmann code CLASS [36, 37] and the Monte Carlo public code Monte Python [38] to analyse the CMB data sets discussed in section 2 when for the selected model there are no posterior samples officially provided by the Planck collaboration. We modify the codes to include the parametrized extra dark radiation (section 4.2) and the three additional parameters to the Planck “base” model². We adopt uniform priors for all the parameters, except for ΔN_{eff} , for which we sample ΔN_{eff}^2 (see section 4.2). We only set a lower limit in the sampling range for A_s, n_s, τ and ΔN_{eff} (0.0 in all cases but for τ , which is 0.04). The prior in τ has virtually no effect on the reported constraints and is justified by observations of the Gunn–Peterson effect, see e.g., Ref. [39]. Our sampling method of choice when CMB data are involved is the Metropolis Hastings algorithm; we run sixteen Monte Carlo Markov Chains (MCMC) for each ensemble of data sets until the fundamental parameters reach a convergence parameter $R - 1 < 0.03$, according to the Gelman-Rubin criterion [40].

When interpreting the low redshift probes of the expansion history (see section 5), we use a different methodology. We aim to reconstruct $H(z)$ (the main observable related with the expansion of the Universe) in the most model-independent way possible, but still requiring a smooth expansion history. For this reason the Hubble function is expressed as piece-wise natural cubic splines in the redshift range $0 \leq z \leq 1.3$. We specify the spline function $H^{\text{recon}}(z)$ by the values it takes at N “knots” in redshift. These values uniquely define the piecewise cubic spline once we ask for continuity of $H^{\text{recon}}(z)$ and its first and second derivatives at the knots, and two boundary conditions. We require the second derivative to vanish at the exterior knots. Thus, our free parameters are the values of $H^{\text{recon}}(z_{\text{knot}})$, where z_{knot} are the redshifts correspondent to the “knots”. We also consider cases in which we vary the sound horizon at radiation drag and the curvature of the Universe (via Ω_k). The location of the knots is arbitrary and we place them at $z = [0, 0.2, 0.57, 0.8, 1.3]$ to match the BAO data constraining power and encompass the SNeIa redshift range. When SNeIa are not included, we limit the fit of $H^{\text{recon}}(z)$ to the range $0 \leq z \leq 0.8$ (and vary one less parameter).

We set uniform priors for all the parameters, with limits which are never explored by the MCMC. We use the public `emcee` code [41], which implements the Affine Invariant Markov Ensemble sampler as sampling method [42] to fit the splines to the cosmological measurements discussed in the previous section. To obtain the likelihood of each position in the parameter space, we integrate the correspondent $H^{\text{recon}}(z)$ to compute $D_V(z)$ and luminosity distance $D_L(z)$ and calculate the χ^2 for BAO and SNeIa, respectively. In addition, we fit $H^{\text{recon}}(z = 0)$ to the direct measurement of H_0 . We run 500 walkers for 10000 steps each and remove 400 steps from each walker (as burn-in phase), as this interval corresponds to several autocorrelation times. By that time, the mean sequence value has been varying around the true mean for much more steps than the needed to reach this regime.

In section 5.1, we quantify the tension between the different joint constraints on the plane H_0 - r_s following [10]. This method is based on the evidence ratio of the product of the distributions with respect to the –ideal–, and ad hoc– case when the maxima of the posteriors coincide (maintaining shape and size).

²The Planck “base” model is a flat, power law power spectrum Λ CDM model with three neutrino species, with total mass 0.06eV)

Then, if we call P_A to the posterior of the experiment A and \mathcal{E} to the ‘unnormalized’ evidence, and with a bar we refer to the shifted case,

$$\mathcal{T} = \frac{\bar{\mathcal{E}}|_{\max A = \max B}}{\mathcal{E}} = \frac{\int \bar{P}_A \bar{P}_B dx}{\int P_A P_B dx}. \quad (3.1)$$

\mathcal{T} is the degree of tension and can be interpreted in the modified Jeffrey’s scale. The odds for the null hypothesis (i.e. both posteriors are fully consistent) are $1 : \mathcal{T}$.

4 Modifying early Universe physics: effect on H_0 and r_s

It is well known that there are two promising ways to alter early cosmology so that the tension between CMB-inferred value and measured value of H_0 is reduced. These are changing the early time expansion history and changing the details of recombination.

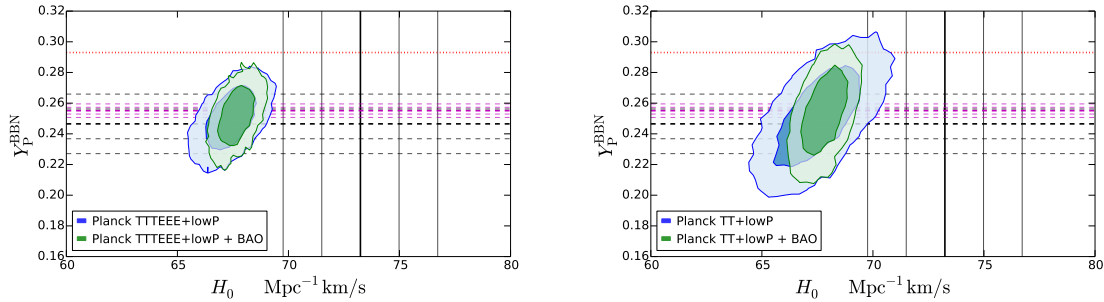


Figure 2. 68% and 95% confidence joint constraints in the H_0 - Y_P^{BBN} parameter space for Planck 2015 using temperature and polarization power spectra (left) and without include high ℓ polarization data (right). The vertical bands correspond to the local H_0 measurement [20]. The horizontal black dashed lines correspond to the measurement (mean and 1 and 2 σ) of the primordial abundance of [43], and in magenta of [44], both from chemical abundances in metal-poor HII regions. The red dotted horizontal line is the 2 σ upper limit of the recent measurement of initial Solar helium abundance of [45].

4.1 Changing the details of recombination: Y_P^{BBN}

Changes in the details of nucleosynthesis can be captured by changes in the primordial Helium mass fraction. The mass fraction in Helium in the early Universe is parametrised by Y_P^{BBN} . In the standard analyses, since the process of standard big bang nucleosynthesis (BBN) can be accurately modelled and gives a predicted relation between Y_P^{BBN} , the photon-baryon ratio, and the expansion rate, the value of Y_P^{BBN} is computed consistently with BBN for every model sampled.

One can also relax any BBN prior and let Y_P^{BBN} vary freely, instead of fixing it to the BBN prediction. The primordial helium fraction has an influence on the recombination history and affects CMB anisotropies mainly through the redshift of last scattering and the diffusion damping scale. The effect of this extra degree of freedom on the inferred value of H_0 can be seen in figure 2. In the H_0 - Y_P^{BBN} parameter space we show 68% and 95% confidence regions for the joint constraints from Planck 2015 data (obtained using the publicly released Planck team’s MCMC), the local H_0 measurement [20], and the measurements (mean and 1 and 2 σ) of the primordial abundance of [43] and [44] (which is less conservative) from chemical abundances in metal-poor HII regions. We also show the conservative 95% upper limit of the measured initial Solar helium abundance of [45].

It is clear that a different value of primordial helium abundance than the measured one would not fix the H_0 tension. Even varying Y_P^{BBN} without a BBN prior, the joint H_0 - Y_P^{BBN} constraints are in a $\sim 2.7\sigma$ disagreement (when using lowTEB, high ℓ TT and polarisation) with the new measurement

of H_0 [20]. If high ℓ polarization data is not included, the tension is reduced because of the larger error bars. However, the constraints from Planck are not in agreement with both H_0 and primordial abundance measurements at the same time, even considering the more conservative measurement of [43].

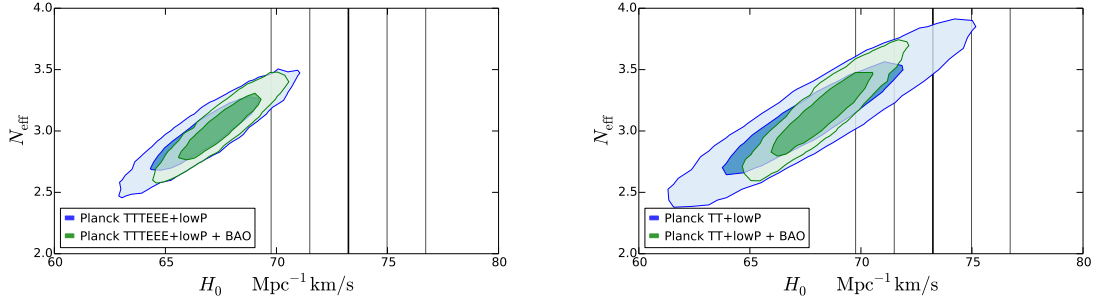


Figure 3. Confidence regions (68% and 95%) of the joint constraints in the H_0 - N_{eff} parameter space for Planck 2015 data (blue) and Planck 2015 + BAO data (green) using full temperature and polarization power spectra (left) and without including high ℓ polarization data (right). Here all species behave like neutrinos when perturbations are concerned. The vertical bands correspond to the local H_0 measurement [20].

4.2 Chainging early time expansion history: ΔN_{eff}

Changes on the early time expansion history are usually enclosed in the parameter N_{eff} : the effective number of neutrino species. For three standard neutrinos $N_{\text{eff}} = 3.04^3$ [46]. In fact light neutrinos are relativistic at decoupling time and they behave like radiation: changing N_{eff} changes the percentage of the Universe’s components that behave like radiation, changing therefore the early expansion history. This has been called “dark radiation” but it can mimic several other physical effects see e.g., [47–58]. For example a model such as the one proposed in [49] of a thermalized massless boson, has a ΔN_{eff} between ~ 0.57 and 0.39 depending on the decoupling temperature [3].

If we define ΔN_{eff} as $N_{\text{eff}} - 3.04$, it is well known that a $\Delta N_{\text{eff}} > 0$ would increase the CMB-inferred H_0 value, bringing it closer to the locally measured one. This can be appreciated in Fig. 3, where we show the results of Planck 2015 for a model where N_{eff} is an additional free parameter and the extra radiation behaves like neutrinos. In the H_0 - N_{eff} parameter space we show the joint 68% and 95% confidence regions for Planck 2015 data (blue) and Planck 2015 + BAO data (green) obtained from the Planck team’s public chains, both using polarization and temperature power spectra (left) or just temperature power spectrum (right). The vertical bands correspond to the local H_0 measurement [20].

A high value of N_{eff} ($\Delta N_{\text{eff}} \sim 0.4$) would alleviate the tension in H_0 and still be allowed by the Planck low TEB and high ℓ temperature power spectra and BAO data as pointed out in [20]. The “preliminary” high ℓ polarization data, disfavours such large ΔN_{eff} ($\sim 2\sigma$ regime), as polarization constrains strongly the effective number of relativistic species.

This is however not the full story. State-of-the-art CMB data have enough statistical power to measure not just the effect of this N_{eff} on the expansion history but also on the perturbations. Neutrino density/pressure perturbations, bulk velocity and anisotropic stress are additional sources for the gravitational potential via the Einstein equations (see e.g., [59–61]). The effect on the perturbations is described by the effective parameters sound speed and viscosity c_s^2 , c_{vis}^2 [62–65]. Neutrinos have $\{c_s^2, c_{\text{vis}}^2\} = \{1/3, 1/3\}$, but other values describe other physics, for example a perfect relativistic fluid will have $\{1/3, 0\}$ and a scalar field oscillating in a quartic potential $\{1, 0\}$. Different values of c_s^2 and c_{vis}^2 would describe other dark radiation candidates. This parametrisation is considered

³The number of (active) neutrinos species is 3, the small correction accounts for the fact that the neutrino decoupling epoch was immediately followed by e^+e^- annihilation.

flexible enough for providing a good approximation to several alternatives to the standard case of free-streaming particles e.g., [66, 67].

Recent analyses have shown that if all N_{eff} species have the same effective parameters c_s^2, c_{vis}^2 , Planck data constraints are tight [3, 68]: $c_s^2 = 0.3240 \pm 0.0060$, $c_{\text{vis}}^2 = 0.327 \pm 0.037$ (with fixed $N_{\text{eff}} = 3.046$; Planck 2015). Moreover, the N_{eff} constraints are not significantly affected compared to the standard case: $N_{\text{eff}} = 3.22^{+0.32}_{-0.37}$ ([68]) against $N_{\text{eff}} = 3.13 \pm 0.31$ (Planck 2015) at 68% confidence level, both using CMB temperature data and CMB lensing. We update the results of [68] by using Planck 2015 power spectra (lowTEB + high ℓ TTTEEE) instead of Planck 2013. Results can be seen in table 2. Using state-of-the-art observations, the constraints on N_{eff} are even tighter, the constraints on c_s^2 and c_{vis}^2 are driven by the high ℓ polarisation data and the N_{eff} constraints are made tighter compared to those in [68] by the high ℓ polarisation data. As the polarisation analysis is “preliminary” these results should be considered preliminary too. In all the cases studied, there is no significant shift in the central value of H_0 . There is no evidence for the main component of the relativistic species behaving differently from a standard neutrino, and this extension does not alleviate the tension in H_0 significantly (tension is reduced only because extending the model results in a slightly larger uncertainty in H_0).

	N_{eff}	c_s^2	c_{vis}^2	H_0
lowTEB+TTTEEE	2.96 ± 0.23	0.324 ± 0.006	0.33 ± 0.04	67.2 ± 1.9
lowTEB + TTTEEE+ lensing	2.91 ± 0.21	0.325 ± 0.006	0.33 ± 0.04	67.0 ± 1.8
lowTEB + TTTEEE+lensing+BAO	2.94 ± 0.18	0.325 ± 0.006	0.33 ± 0.04	67.2 ± 1.3

Table 2. Marginalised mean and 68% confidence for the parameters of interest for the different combinations of data.

The fact that when leaving c_s^2, c_{vis}^2 as free parameters in the analysis one recovers tight constraints consistent with $\{1/3, 1/3\}$ and $N_{\text{eff}} = 3.04$ is a good confirmation of the existence of a cosmic neutrino background. However, this does not exclude the possibility of the existence of extra relativistic species (i.e., dark radiation) with different behaviour than neutrinos. Their presence could be masked in the analysis by the dominant component, the cosmic neutrino background. Thus next, we shall assume that there are three neutrino families in the Universe (i.e., that the 3.04 effective species have $\{c_s^2, c_{\text{vis}}^2\} = \{1/3, 1/3\}$) and that any extra dark radiation ΔN_{eff} component has free effective sound and viscosity parameters. We have modified the publicly available CLASS code [36, 37] to implement this. In figure 4 we show the qualitative effects on the CMB power spectra of the parameters describing this extra dark radiation component.

Given that for $\Delta N_{\text{eff}} \sim 0$ there is almost no difference in the likelihood for different values of c_s^2 and c_{vis}^2 , the MCMC tend to be stuck in that zone of the parameter space⁴. To prevent it, we sample ΔN_{eff}^2 instead. We find that, once 3.046 standard neutrinos are fixed, the presence of extra relativistic species, even giving freedom to the behaviour of their perturbations, is not favoured by the data. The results are summarized in table 3, with the upper limits of ΔN_{eff} at 95% of confidence level. The joint constraints on ΔN_{eff} and H_0 are shown in figure 5.

The constraints on c_{vis}, c_s are very weak because of the strong upper limit on ΔN_{eff} .

Should the low-level systematic present in the polarisation data be found to be sub-dominant in the published error-budget, this finding implies that there is not much room for an extra component in the early universe whose density scales with the expansion like radiation but whose perturbations have the freedom to behave like a perfect fluid, a neutrino, a scalar field or anything in between. This offers a useful confirmation of one of the key the standard assumptions on which the standard cosmological model is built. Also in this more general model, of the CMB data, it is the high- ℓ polarisation what disfavors high values of H_0 .

⁴For the parameters c_{vis}^2 and c_s^2 we limit the sampling to the range $[0.0, 1.1]$. That is because values higher than one are not physical and this way we also optimize the performance of the analysis, since we do not explore the parameter space where this values are allowed to be very large in the region close to $\Delta N_{\text{eff}} = 0$.

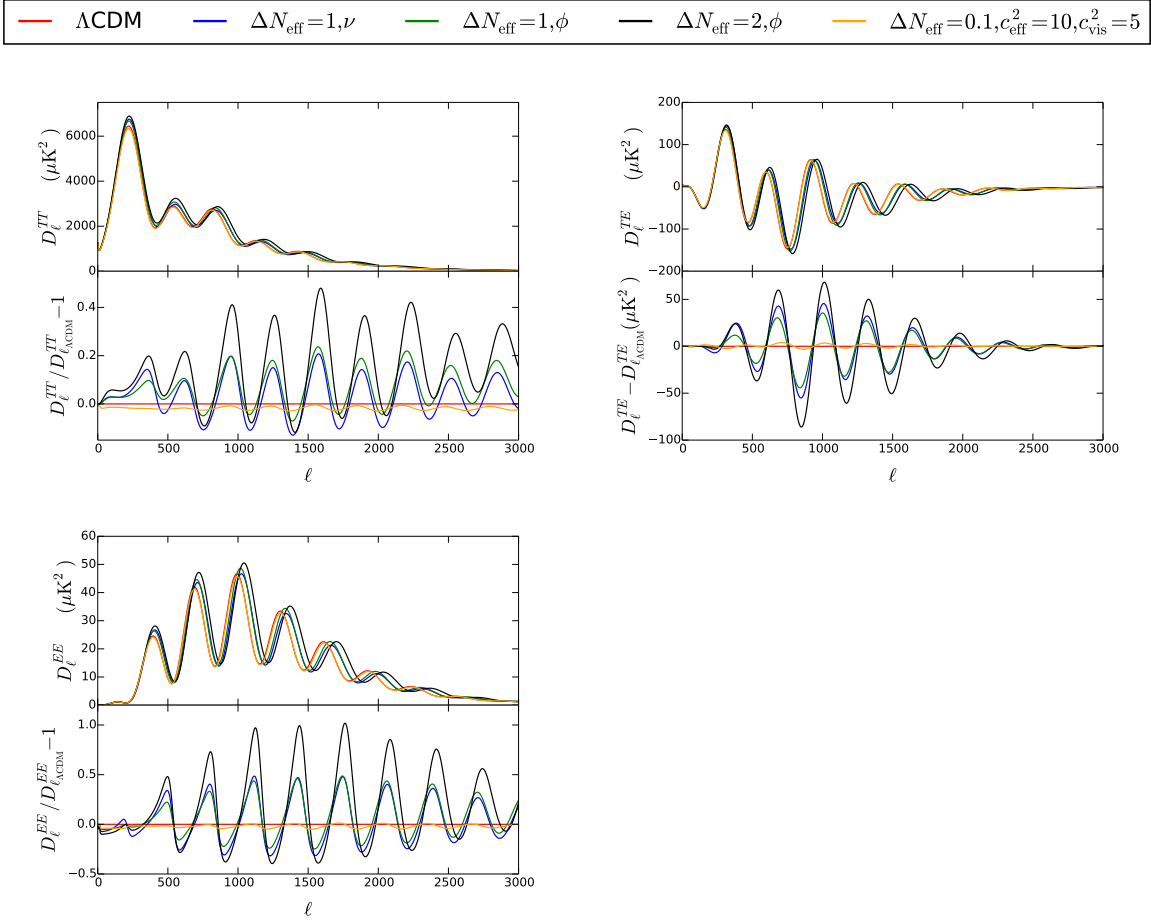


Figure 4. CMB temperature (*left*), temperature and polarization cross correlation (*right*) and polarization (*bottom*) power spectra predictions for Λ CDM (red) and the following extensions: one more neutrino (blue), one scalar field (green), two scalar fields (black) and a illustrative case with extreme (non physical) values of c_s^2 and c_{vis}^2 with $\Delta N_{\text{eff}} = 0.1$ (orange).

	ΔN_{eff}	c_s^2	c_{vis}^2	H_0
lowTEB+ TTTEEE	< 0.36	0.25 ± 0.11	0.48 ± 0.32	$68.7^{+1.3}_{-0.7}$
lowTEB+ TTTEEE+CMB lensing	< 0.33	0.28 ± 0.13	0.49 ± 0.33	$69.0^{+1.0}_{-0.9}$
lowTEB+ TTTEEE+CMB lensing+BAO	< 0.28	0.31 ± 0.14	0.51 ± 0.35	$68.8^{+0.6}_{-0.7}$
lowTEB+ TT	< 0.67	0.32 ± 0.16	0.58 ± 0.47	$68.6^{+3.1}_{-0.8}$
lowTEB+ TT+CMB lensing	< 0.63	0.35 ± 0.19	0.62 ± 0.32	$69.9^{+1.7}_{-1.9}$
lowTEB+ TT+CMB lensing+BAO	< 0.31	0.44 ± 0.27	0.55 ± 0.52	$68.6^{+0.8}_{-0.7}$

Table 3. Marginalised constraints for the parameters of interest for the different combinations of data. We report the the upper limit for ΔN_{eff} (95% confidence level), the mean and the 68% confidence level errors for c_s^2 and c_{vis}^2 and the highest posterior density intervals for H_0 .

5 Changing late-time cosmology

The CMB is sensitive to both late and early cosmology. When fitting the CMB power spectrum simultaneous assumptions about the early and late cosmology must be made, with the implication that the physics of both epochs are entwined in the resulting constraints. Then, it is difficult to determine

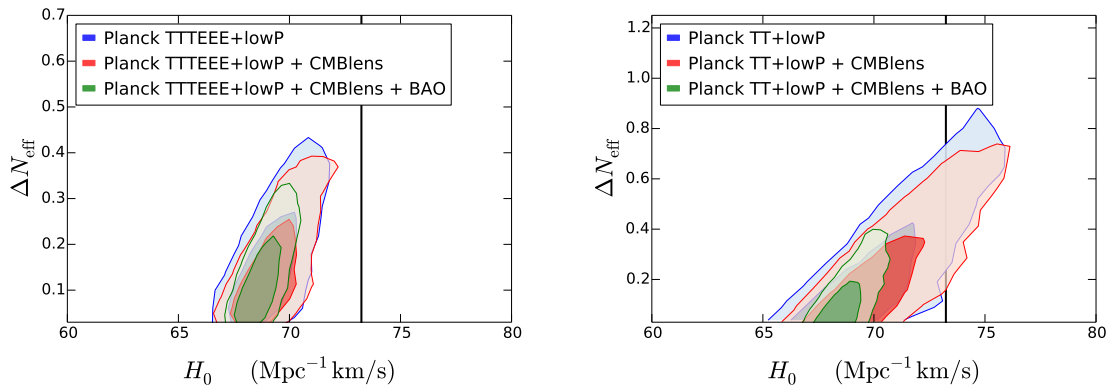


Figure 5. Marginalized 68% and 95% confidence level constraints in the $\Delta N_{\text{eff}}-H_0$ plane. *Left:* Planck data including full temperature and polarization power spectra. *Right:* Excluding high ℓ polarisation. We report results using Planck 2015 power spectra (blue), adding CMB lensing (red) and adding also BAO (green). The vertical black bands correspond to the local H_0 measurement [20]. Note the change in the scale of the y axis in each plot.

what physics beyond Λ CDM would be the responsible of possible deviations from the model. Exploring non-standard late cosmology evolution, possibly in a minimally-parametric or model independent way is in general complicated if CMB constraints are to be included. Nevertheless, although not including CMB constraints makes the analysis much easier, it would not be competitive nor interesting (as one of the best cosmological probe we have is being ignored). There is however a way to analyse CMB data so that it is sensitive only to early cosmology as shown in [69–71]: the resulting constraints do not depend on late-time physics and can therefore be included when analysing late-time data in a model-independent way. The latest CMB Planck data were analysed in this way in [33], where a variety of models of the early Universe are studied. Here we use the results –obtained assuming standard early-time physics (i.e. a flat Universe composed of baryons, radiation, standard neutrinos, cold dark matter and dark energy in the form of cosmological constant from deep in the radiation era down to recombination)– in the form of a constraint on the sound horizon at radiation drag: $r_s^{\text{early}} = 147.00 \pm 0.34$ Mpc.

As it is explained in section 3, we aim to reconstruct $H(z)$ in the most model independent way possible and also to calibrate the anchors for the distance ladder. We use BAO and SNeIa data along with the measured value of H_0 and r_s^{early} . The only assumptions made are that the expansion history of the Universe is smooth and continuous, that the spatial section of the Universe is flat, that SNeIa form an homogeneous group such as they can be used as standard candles and that the sound horizon at radiation drag, r_s , is a standard ruler which calibrates the cosmic distance scale given by BAO observations ([6, 27, 28]). We also consider the case in which the assumption about the geometry of the Universe is relaxed (see section 5.2). With this minimal assumptions, H_0 and r_s are treated only as the calibration of the cosmic distance ladder and they are related by $H_0 r_s = \text{constant}$. Usually r_s is determined from CMB data. While in the standard analysis this relies on several assumptions, by using the results of [33] as our r_s prior, we make this measurement independent from late-time physics assumptions.

Without any assumption about the geometry of the Universe, the comoving distance χ is related to the Hubble parameter by

$$\chi(z) = \frac{c}{H_0 \sqrt{|\Omega_k|}} \mathcal{S}_k \left(\sqrt{|\Omega_k|} H_0 \int_0^z \frac{dz'}{H(z')} \right), \quad (5.1)$$

where $\mathcal{S}_k(x) = \sinh(x)$, x or $\sin(x)$ for $\Omega_k > 0$, $= 0$ or < 0 , respectively. Then, the angular diameter

Data sets	$H(z=0)$	$H(z=0.2)$	$H(z=0.57)$	$H(z=0.8)$	$H(z=1.3)$	r_s	ΔM
$H_0 + \text{BAO} + r_s^{\text{early}}$	72.3 ± 1.7	72.9 ± 1.9	96.4 ± 2.5	102.5 ± 14.0	—	—	—
$H_0 + \text{SN}$	73.2 ± 1.8	81.0 ± 2.5	99.3 ± 4.4	107.0 ± 9.0	161.9 ± 73.1	—	0.10 ± 0.06
$H_0 + \text{BAO} + r_s^{\text{early}} + \text{SN}$	69.4 ± 1.0	75.5 ± 1.2	94.0 ± 1.8	101.2 ± 6.2	150.1 ± 62.9	—	-0.03 ± 0.03
$H_0 + \text{BAO}(\ast) + \text{SN}$	73.1 ± 1.8	80.6 ± 2.4	101.5 ± 3.8	109.3 ± 7.6	143.7 ± 59.7	136.8 ± 4.0	0.10 ± 0.06
$H_0 + \text{BAO} + r_s^{\text{early}} + \text{SN}(\circ)$	$69.6^{+1.1}_{-1.3}$	75.6 ± 1.2	94.0 ± 4.1	101.1 ± 11.2	147.1 ± 89.3	—	-0.03 ± 0.04
$H_0 + \text{BAO}(\ast) + \text{SN}(\circ)$	$73.4^{+1.5}_{-2.0}$	83.0 ± 3.0	111.9 ± 8.9	130.0 ± 17.8	237.9 ± 123.4	133.0 ± 4.7	0.10 ± 0.06
$\text{BAO} + r_s^{\text{early}} + \text{SN}(\circ)$	$66.3^{+1.7}_{-1.7}$	75.1 ± 1.1	101.2 ± 5.7	118.1 ± 13.9	215.9 ± 112.0	—	-0.11 ± 0.05

Table 4. Marginalized mean and 68% confidence regions for the parameters included in the reconstruction for each of the combinations of data sets we consider. When reporting asymmetric errors, we report the highest posterior density value for H_0 . The last column corresponds to ΔM , the offset in the absolute magnitude compared with the standard value. We report it here to show that the supernovae absolute magnitude is not significantly shifted away from its value determined internally by external the data. the “*” symbol indicate that no CMB-derived r_s prior is used. The symbol “o” indicates that Ω_k is left as a free parameter.

distance and the luminosity distance are

$$D_A(z) = \frac{\chi(z)}{(1+z)}, \quad D_L(z) = (1+z)\chi(z). \quad (5.2)$$

BAO observations provide measurements of D_V , which is related to $H(z)$ by

$$D_V(z) = \left[cz(1+z)^2 D_A(z)^2 H(z)^{-1} \right]^{1/3} = \left[cz \left(\int_0^z \frac{cdz'}{H(z')} \right)^2 H(z)^{-1} \right]^{1/3}. \quad (5.3)$$

While it is customary to parametrise dark energy properties via the equation of state parameter $w(z)$, it should be evident that the observable quantity is $H(z)$. Afterwards, to convert $H(z)$ into a $w(z)$ a model for dark energy must be assumed as well as a value for Ω_m :

$$H(z) = (1+z)^{3/2} \sqrt{\Omega_m + \Omega_{\text{DE}} \exp \left[3 \int_0^z \frac{w(z')}{1+z'} dz' \right]}, \quad (5.4)$$

here Ω_{DE} is the density parameter for the dark energy and flatness is assumed.

For our model-independent reconstruction of the late-time expansion history where the Hubble parameter is expressed in piece-wise natural cubic splines, $H(z)$ is specified by the values it takes at N “knots” in redshift; $N = 4$ for BAO only analysis and $N = 5$ when SNeIA are included. This parametrisation allows for smooth and relatively generic expansion histories. As indicated in [35] for the compressed data set of supernovae, we allow an offset in the absolute magnitude compared with the standard value, ΔM , treated as a free (nuisance) parameter.

We summarize the results of our analysis (mean and 68% confidence intervals) in table 4. In the following figures (figures 6-8) we show the best fit of our reconstruction of $H(z)$ (black line), the 68% confidence region obtained by plotting the curves corresponding to 500 points of the chain randomly selected from the 68% with highest likelihood (red) and the Hubble parameter corresponding to the Λ CDM prediction using the best fit values of Planck 2015 with lensing [3] (blue). The dashed blue line is the Λ CDM prediction using $H_0 = 73.0 \text{ km s}^{-1} \text{ Mpc}^{-1}$ instead of the Planck 2015 inferred value. In the plots, data are shown in green and the predictions of the observables using $H^{\text{recon}}(z)$ in black (bestfit) and red (68% region). In this case we show ratios with respect Λ CDM prediction for clarity. The vertical grey lines mark the position of the “knots”.

Figure 6 shows the reconstruction of $H^{\text{recon}}(z)$ and $D_V(z)$ for the analysis of BAO and H_0 [20] data with the r_s^{early} prior. While in a Λ CDM model $H(z)$ is monotonically increasing with redshift, here $H^{\text{recon}}(z)$ is almost constant in the range $0 < z < 0.2$ to match the local H_0 determination to the distance measurements which are “anchored” by r_s^{early} , predicting a sharper acceleration at low redshift. Given that the lowest redshift sampled by the BAO data is $z = 0.106$, H_0 is determined mostly by the direct measurement of [20]. Using the formalism described in section 3, we can quantify

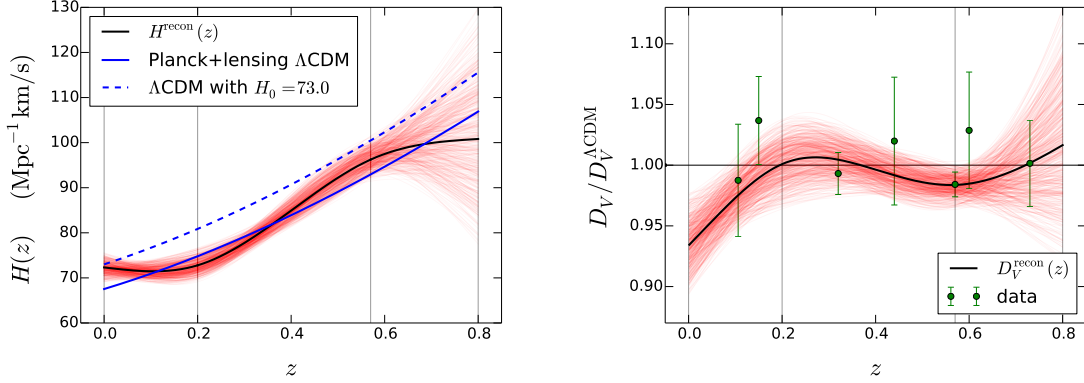


Figure 6. *Left:* Results of the reconstruction of $H(z)$ using the direct measurement of H_0 of [20] and the BAO data set. *Right:* BAO data included in the reconstruction. We plot $(D_V/r_s)r_s^{\text{early}}$ data points and the D_V obtained with the corresponding $H^{\text{recon}}(z)$.

the significance of this feature with respect to the Planck 2015 ΛCDM $H(z)$ distribution. We consider various redshifts ($z = 0, 0.2$ and 0.57 which we select to coincide with the knots) yielding a multivariate distribution. With this choice the odds are 1:49. Although the results would be different depending on the chosen redshifts, we consider that this choice is representative and the results will not vary qualitatively with another reasonable choice. This apply for all the cases studied here.

In figure 7 we show the results for the reconstruction of $H(z)$ using SNIa and H_0 . We show $H^{\text{recon}}(z)$ and the distance modulus. The redshift sampling of SNIa data is much denser than BAO: this constrains the shape of $H^{\text{recon}}(z)$, but not the normalisation (as the analysis marginalises over the supernovae absolute magnitude) which is anchored at $H_0 \sim 73 \text{ km/s/Mpc}$ by the H_0 measurement. The reconstructed shape is very close to the ΛCDM until the data sampling is sparser ($z \gtrsim 0.6$) and errors grow. The odds of SNIa reconstructed $H(z)$ shape compared to the one obtained using only BAO, H_0 and r_s^{early} are 1:52.

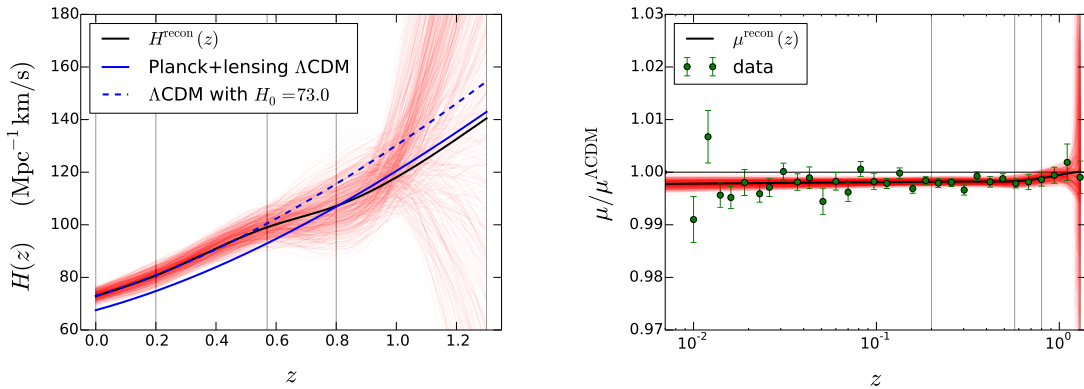


Figure 7. *Left:* Results of the reconstruction of $H(z)$ using the direct measurement of H_0 of [20] and the SNIa data set. *Right:* SNIa data included in the reconstruction (green). We plot the distance modulus, μ , obtained with the corresponding $H^{\text{recon}}(z)$. The plotted errorbars correspond to the square root of the diagonal of the covariance matrix (we account correctly for the actual correlation among bins in the analysis).

Finally, when using the combination H_0 , SNIa and BAO with our r_s^{early} prior (figure 8), SNIa observations constrain the shape of $H^{\text{recon}}(z)$ but the normalization tries to fit H_0 and BAO (via r_s^{early}) at the same time. The H_0 measurement has a 2.4% error, but the r_s^{early} determination a 0.23%

error: the statistical power of the BAO normalisation shifts the recovered $H^{\text{recon}}(z=0)$ to lower values compared to the local determination (and closer to the Planck-inferred value under a Λ CDM model). Remarkably, given the freedom that the cubic splines have, our reconstruction of $H(z)$ is close to the Λ CDM prediction. In this case, the odds compared to the shape obtained using only BAO and H_0 are 1:6, as this is a intermediate solution between the standard Λ CDM shape with low H_0 and the wiggly reconstruction obtained above.

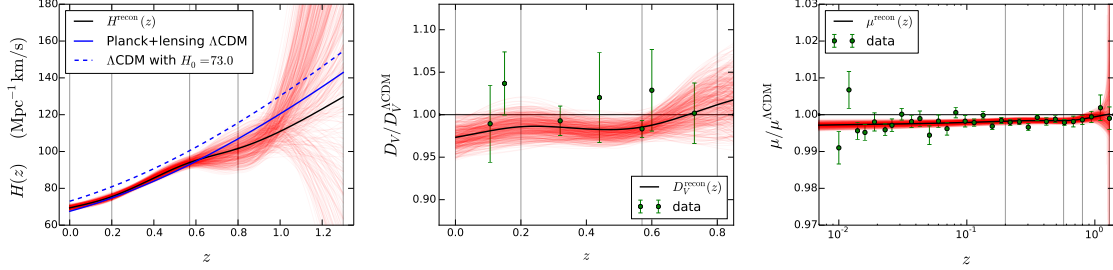


Figure 8. *Left:* Results of the reconstruction of $H(z)$ using the direct measurement of H_0 of [20], BAO and SNeIa data set with a CMB-derived r_s prior. *Middle and right:* Observational data included in the reconstruction (green), as in the previous cases, and the prediction using the corresponding $H^{\text{recon}}(z)$.

To summarise, when using the local H_0 measurement and BAO data normalised to the CMB-derived r_s^{early} under standard early Universe assumptions, the reconstruction indicates a sharp increase in the cosmic acceleration rate ($H(z) \sim \text{constant}$) at $z < 0.2$, where the BAO data have little statistical power. A dark energy equation of state parameter $w < -1$ (or dropping recently below -1) would fit the bill. However, when including SNeIa the shape of the expansion history is constrained not to deviate significantly from that of Λ CDM (at $z < 0.6$ where there are many data points) and thus only the normalisation can adjust, taking a value intermediate between the low and high redshift “anchors”, as $H_0 r_s = \text{constant}$. Thus a phantom dark energy is not favoured by the data.

Relaxing the flatness assumption does not change the results qualitatively (see sec. 5.2).

5.1 Reconstruction independent from the early-time physics

To remove the dependence on the early Universe assumptions introduced by the high redshift BAO anchor, we now treat r_s as a free parameter in our analysis without including the prior of the early Universe of r_s^{early} . We consider the data set combination H_0 , BAO(*) and SNeIa (hereafter the “*” symbol indicate that no CMB-derived r_s^{early} prior is used).

This is illustrated in Fig. 9. The low redshift standard ruler measurement constrains the combination $r_s h$ which is reported here as a band in the H_0 - r_s plane. This constraint only relies on the BAO yielding a standard ruler (of unknown length), on SNe being standard candles (of unknown luminosity) spatial flatness and on a smooth expansion history. The local H_0 measurement or the early-time r_s “anchors” can be used to break the degeneracy. The r_s measurement relies on early-time physics assumptions (i.e. the value of N_{eff} , Y_P , recombination physics, epoch of matter-radiation equality etc.). The H_0 measurement relies on local calibrators of the cosmic distance ladder.

The constraints on our parameters are reported in table 4 and the reconstruction results are shown in figure 10, using the same conventions as in previous plots. Once we free the CMB-anchor of BAO (no r_s prior) the reconstruction is similar to that with only SNeIa: $H^{\text{recon}}(z)$ is very similar to the Λ CDM prediction (with $H_0 \sim 73$). $H^{\text{recon}}(z=0)$ is in $\sim 2.9\sigma$ tension with the value obtained by Planck 2015, which assumes Λ CDM. This procedure yields a model-independent estimate of $r_s = 136.7 \pm 4.1$; remarkably, with an error small enough to raise a tension of 2.6σ with Planck 2015-derived value assuming Λ CDM, and 2.5σ if we compare with r_s^{early} of [33]. This tension in r_s between the model independent measurement and the CMB-inferred value is entirely due to the tension in H_0 , via the relation $H_0 r_s = \text{constant}$. As in previous cases, this data combination disfavors a recent sharp acceleration given by the shape of $H^{\text{recon}}(z)$ using H_0 and BAO, with odds of 1:65.

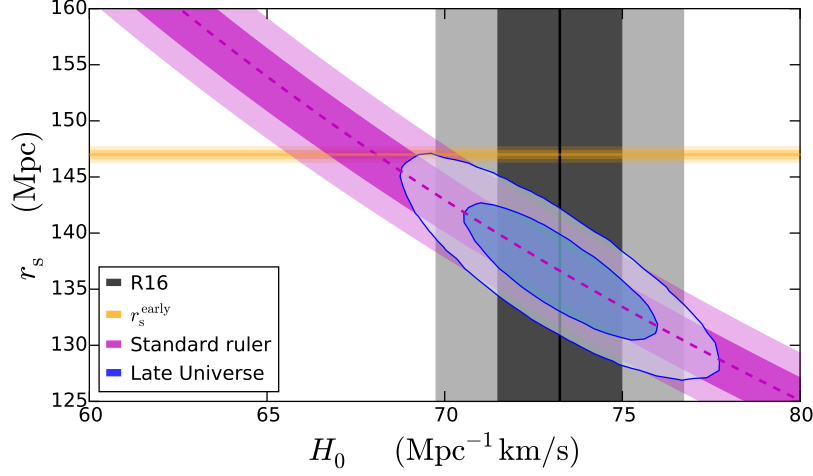


Figure 9. Without an absolute distance scale, such as an H_0 determination, the low redshift standard ruler measurement constrains the combination $r_s h$, and thus $r_s H_0$ which appears as a (purple) band. The local H_0 measurement (gray) can be used to break the degeneracy (yielding the blue confidence regions).

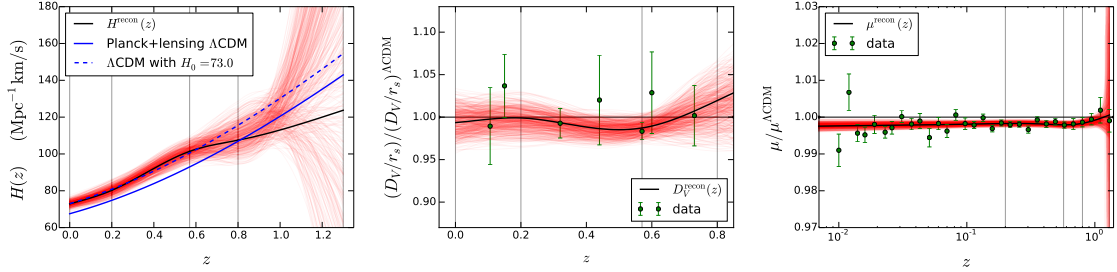


Figure 10. *Left:* Reconstructed of $H(z)$ using the direct measurement of H_0 of [20], BAO(*) and SNeIa data set and letting r_s vary as a free parameter. *Middle and right:* Observational data included in the reconstruction (green), as in previous cases, and the prediction using the corresponding $H^{\text{recon}}(z)$.

It is interesting to note that the reconstructed *shape* of $H^{\text{recon}}(z)$ is constrained to be very close to the Λ CDM-predicted shape. This is illustrated in figure 11 for the combination Supernovae, BAO and H_0 : the maximal deviations at $z < 0.6$ where the data have most of their statistical power, are at the 5% level.

For completeness, in figure 12, we show different CMB constraints on r_s compared with our measurement (black bands). Only when N_{eff} is free and only Planck temperature data is used, the constraint is modestly consistent ($\sim 2\sigma$). In the other cases, the tension is significant, except for the analysis of Planck 2015 temperature power spectrum limited to $\ell \geq 1000$ [23]. However, as discussed by these authors, most of the parameters obtained using only this ℓ range are in tension with Planck 2015 $\ell < 1000$ and WMAP9 constraints. Note that the tensions in each case (in parenthesis in figure 12) are very similar in most of the cases although by eye it may not obviously appear. This is because the error on the low redshift determination is much larger and dominates the comparison.

It is illustrative to show the joint constraints for H_0 and r_s , which we do in figure 13. The vertical band is the local H_0 measurement and the blue contours are the constraints obtained in this work. As said before, H_0 and r_s are related by $H_0 r_s$ and they are perfectly anticorrelated in our measurement. Here the perfect degeneracy is lifted by the measurement of H_0 . In the same way, if the prior r_s^{early} is

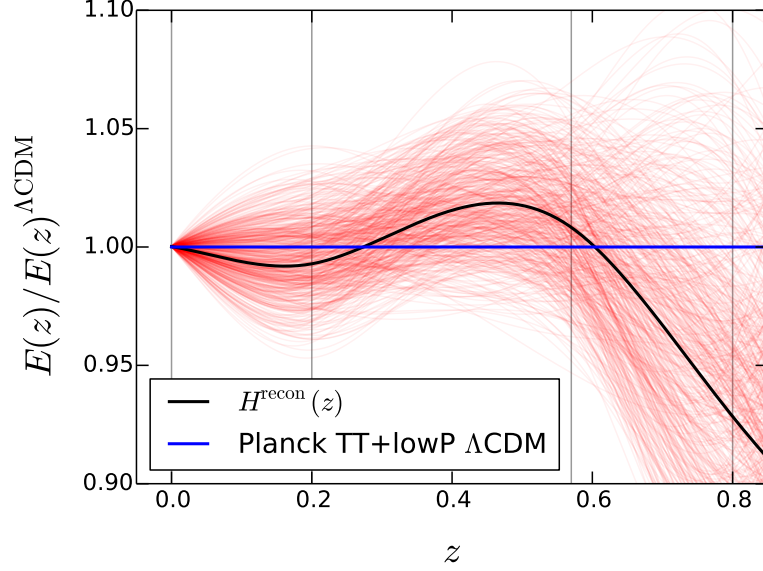


Figure 11. Reconstructed shape of the expansion history $E(z) = H(z)/H_0$, normalised to a standard Λ CDM expansion (with Planck-inferred density parameters), each with its corresponding value of H_0 . At $z < 0.6$ where the data have most statistical power, maximal deviations are at the 5% level.

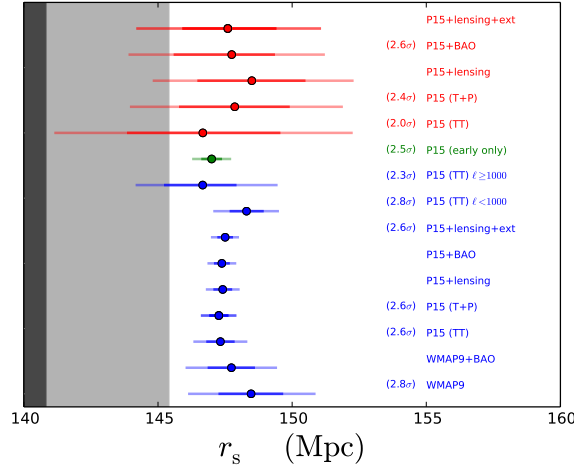


Figure 12. Marginalised 68% and 95% constraints on r_s for different analysis of CMB data, obtained from Planck Collaboration 2015 public chains [3], WMAP9 [1] (analysed with the same assumptions than Planck) and the results of the work of [23] (TT, $\ell > 1000$ and $\ell < 1000$) and [33] (early only). We show the constraints obtained in a Λ CDM context in blue, Λ CDM+ N_{eff} in red, the constraints obtained by analysing the CMB without any assumption of late universe physics (taken from [33]) in green. The result from this work is shown as a gray band.

included instead H_0 from [20], the constraint on H_0 will be approximately⁵ $H_0^m r_s^m / r_s^{\text{early}} \sim 68$, with

⁵This relation is not exact because the prior r_s^{early} is applied at various redshift and in combination with the BAO measurements.

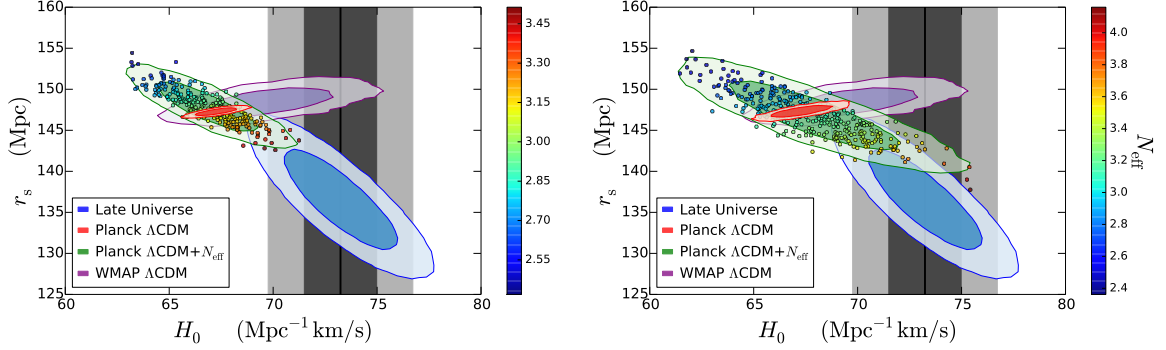


Figure 13. Marginalized constraints in the H_0 - r_s plane (68% and 95% regions) for the cases discussed in the text. Planck data includes high ℓ polarization in the left panel and does not in the right one. Color-coded are the corresponding values of N_{eff} in the case of $\Lambda\text{CDM}+N_{\text{eff}}$.

	$\log \mathcal{T}$	Odds	Jeffrey's modified scale	Gaussian tension
Planck ΛCDM (T+P)	4.75	0.0086 (1:116)	strong	3.7
Planck ΛCDM (TT)	4.31	0.013 (1:76)	strong	3.5
Planck $\Lambda\text{CDM}+N_{\text{eff}}$ (T+P)	3.55	0.029 (1:34)	strong	3.1
Planck $\Lambda\text{CDM}+N_{\text{eff}}$ (TT)	2.02	0.13 (1:8)	positive	2.1
WMAP ΛCDM	3.59	0.027 (1:37)	strong	3.1

Table 5. Two dimensional tension between the low redshift joint constraints on $H_0 - r_s$ and the CMB-derived constraints. See section 3 for details.

the superscript m meaning “measured”, recovering a value of H_0 close to the Planck-inferred value.

We also show the results of Planck using temperature and polarization power spectra (left) and only temperature power spectrum (right) for a ΛCDM model (red) and a model which vary N_{eff} (green); and of WMAP9 for a ΛCDM model (analysed in the same way as Planck, purple). It is possible to appreciate how, as CMB experiments derive constraints assuming a model, the correlation is different and it depends strongly on the adopted model (i.e ΛCDM vs. $\Lambda\text{CDM}+N_{\text{eff}}$).

In table 5, we report the tension in the H_0 - r_s plane between our measurement and CMB experiments for different models (computed as explained in section 3), expressed as $\log \mathcal{T}$, the odds for full consistency and the tensions in σ (computed assuming gaussianity). Only for a model with extra dark radiation and discarding Planck’s high ℓ polarisation data the two constraints are in acceptable agreement (i.e., the tension is not considered strong). From Fig. 13 it is possible to appreciate that within ΛCDM , excluding polarisation data increases the CMB-derived H_0 value, making CMB more consistent with the local H_0 ; however including or excluding polarisation data does not alter significantly the r_s determination. To make the local H_0 determination, the low-redshift estimate of the combination $r_s h$ and the CMB r_s determination fully consistent with each other, r_s should be significantly lowered. Among the ΛCDM extensions we explored the only one that achieves this is allowing $N_{\text{eff}} \sim 3.4$.

5.2 Reconstruction with free curvature

Finally, we also explore the case where the curvature of the Universe is not fixed to $\Omega_k = 0$. In this case we add Ω_k as a free varying parameter to our reconstruction, computing the distances accordingly to equation 5.1. We reconstruct $H(z)$ with BAO and SNeIa data together using r_s^{early} prior and without it. We also consider the case in which the H_0 measurement is not included (using only r_s^{early} to calibrate the distance ladder). Ω_k remains largely unconstrained, and still broadly consistent with

zero. There is no significant shift in the rest of parameters, with the only difference that the error bars are larger. The constraints are summarized in table 4. Given the freedom of our expansion history reconstruction, to obtain useful constraints on Ω_k more data would be needed (see for example, [27, 28] where curvature constraints are reported). In the near future, anisotropic measurements of the BAO feature from on-going and forthcoming surveys could also be used.

6 Discussion and Conclusions

The standard Λ CDM model with only a handful of parameters, provides an excellent description of a host of cosmological observations with remarkably few exceptions. The most notable and persistent one is the local determination of the Hubble constant H_0 , which, with the recent improvement by [20], presents a 3σ tension with respect to the value inferred by the Planck Collaboration (assuming Λ CDM). The CMB is mostly sensitive to early-Universe physics, and the CMB-inferred H_0 measurement thus depends on assumptions about both early time and late-time physics. A related quantity that the CMB can measure in a way that does not depend on late-time physics is the sound horizon at radiation drag, r_s . This measurement however is still model-dependent in that it relies on standard assumptions about early-time physics. On the other hand the local measurement of H_0 is model-independent as it does not depend on cosmological assumptions. As this work was nearing completion, new quasar time-delay cosmography data became available [22]. Within the Λ CDM model these provide an H_0 constraint centered around 72 km/s/Mpc, with a 4% error and thus shows reduced tension.

The two parameters r_s and H_0 are strictly related when we consider also BAO observations. Expansion history probes such as BAO and SNIa can provide a model-independent estimate of the low-redshift standard ruler, constraining directly the combination $r_s h$ (with $H_0 = h \times 100$ km/s/Mpc). Thus r_s and H_0 provide absolute scales for distance measurements (anchors) at opposite ends of the observable Universe. In the absence of systematic errors in the measurements, if the standard cosmological model is the correct model, indirect (model-dependent) and direct (model-independent) constraints on these parameters should agree. The tension could thus provide evidence of physics beyond the standard model (or unaccounted systematic errors).

We have performed a complete cosmological study of the current tension between the inferred value of H_0 from the latest CMB data (as provided by the Planck satellite) [3] and its direct measurement, with the recent update from [20]. This reflects into a tension between cosmological model-dependent and model-independent constraints on r_s .

We first have explored models for deviations from the standard Λ CDM in the early-Universe physics. When including CMB data alone (or in combination with geometric measurements that do not rely on the H_0 anchor such as BAO) we find no evidence for deviations from the standard Λ CDM model and in particular no evidence for extra effective relativistic species beyond three active neutrinos. This conclusion is unchanged if we allow additional freedom in the behaviour of the perturbations, both in all relativistic species or only in the additional ones.

Therefore we put limits on the possible presence of a Universe component which mean energy scales like radiation with the Universe expansion but which perturbations could behave like radiation, a perfect fluid, a scalar field or anything else in between. On the other hand the value for the Hubble constant inferred by these analyses and other promising modifications of early-time physics, is always significantly lower than the local measurement of [20]. Should the low-level systematics present in the high ℓ “preliminary” Planck polarisation data be found to be non-negligible, the TEE data should not be included in the analysis. In this case, including only the “recommended” baseline of low ℓ temperature and polarisation data and only temperature for high ℓ , the tight limits relax and the tension reduces to an acceptable level for a cosmological model with extra dark radiation corresponding to $\Delta N_{\text{eff}} \sim 0.4$. The constraints on the effective parameters which describe the behaviour of the extra radiation in terms of perturbations are too weak to discriminate among the different candidates.

Another possible way to reconcile the CMB-derived H_0 value and the local measurement is to allow deviations from the standard late-time expansion history of the Universe. Rather than invoking specific models we have reconstructed the expansion history in a model-independent, minimally para-

metric way. Our method to reconstruct $H(z)$ does not rely on any model and only require minimal assumptions. These are: SNeIa form a homogeneous group and can be used as standard candles, r_s is a standard ruler for BAO corresponding to the sound horizon at radiation drag, the expansion history is smooth and continuous and the Universe is spatially flat. When only using BAO, and H_0 measurement with an early Universe r_s prior, the reconstructed $H(z)$ shows a sharp increase in acceleration at low redshift, such as that provided by a phantom equation of state parameter for dark energy. However when SNeIa are included, the shape of $H(z)$ cannot deviate significantly from that of a Λ CDM, disfavouring therefore the phantom dark energy solution. When the CMB r_s prior is removed, this procedure yields a model-independent determination of r_s (and the expansion history) without any assumption on the early Universe. The r_s value so obtained is significantly lower than that obtained from the CMB assuming standard early-time physics (2.6σ tension). When we relax the assumption about the flatness of the Universe, the curvature remains largely unconstrained and the error on the other parameters grow slightly. We do not find significant shifts in the rest of the parameters.

Of course this hinges on identifying the BAO standard ruler with the sound horizon at radiation drag. Several processes have been proposed that could displace the BAO feature, the most important being non-linearities, bias e.g., [72, 73] and non-zero baryon-dark matter relative velocity [74–76]. These effects however have been found to be below current errors [77–79] and below the 1% level. It is therefore hard to imagine how these effect could introduce the 5 – 7% shift required to solve the tension.

In summary, because the shape of the expansion history is tightly constrained by current data, in a model-independent way, the H_0 tension can be restated as a mis-match in the normalisation of the cosmic distance ladder between the two anchors: H_0 at low redshift and r_s at high redshift. In the absence of systematic errors, especially in the high ℓ CMB polarisation data and/or in the local H_0 measurement, the mismatch suggest reconsidering the standard assumptions about early-time physics. Should the “preliminary” high ℓ CMB polarisation data be found to be affected by significant systematics and excluded from the analysis, the mismatch could be resolved by allowing an extra component behaving like dark radiation at the background level with a $\Delta N_{\text{eff}} \sim 0.4$. Other new physics in the early Universe that reduce the CMB-inferred sound horizon at radiation drag by $\sim 10\text{Mpc}$ (6%) would have the same effect.

Acknowledgments

We thank Graeme Addison and Alan Heavens for valuable discussion during the development of this study, which helped to improve this work. JLB is supported by the Spanish MINECO under grant BES-2015-071307, co-funded by the ESF. Funding for this work was partially provided by the Spanish MINECO under projects AYA2014-58747-P and MDM-2014- 0369 of ICCUB (Unidad de Excelencia Maria de Maeztu). JLB acknowledges hospitality of Radcliffe Institute for Advanced Study, Harvard University.

Based on observations obtained with Planck (<http://www.esa.int/Planck>), an ESA science mission with instruments and contributions directly funded by ESA Member States, NASA, and Canada.

Funding for SDSS-III has been provided by the Alfred P. Sloan Foundation, the Participating Institutions, the National Science Foundation, and the U.S. Department of Energy Office of Science. The SDSS-III web site is <http://www.sdss3.org/>.

SDSS-III is managed by the Astrophysical Research Consortium for the Participating Institutions of the SDSS-III Collaboration including the University of Arizona, the Brazilian Participation Group, Brookhaven National Laboratory, Carnegie Mellon University, University of Florida, the French Participation Group, the German Participation Group, Harvard University, the Instituto de Astrofísica de Canarias, the Michigan State/Notre Dame/JINA Participation Group, Johns Hopkins University, Lawrence Berkeley National Laboratory, Max Planck Institute for Astrophysics, Max Planck Institute for Extraterrestrial Physics, New Mexico State University, New York University, Ohio State University, Pennsylvania State University, University of Portsmouth, Princeton University, the Span-

ish Participation Group, University of Tokyo, University of Utah, Vanderbilt University, University of Virginia, University of Washington, and Yale University.

References

- [1] G. Hinshaw, D. Larson, E. Komatsu, D. N. Spergel, C. L. Bennett, J. Dunkley, M. R. Nolta, M. Halpern, R. S. Hill, N. Odegard, L. Page, K. M. Smith, J. L. Weiland, B. Gold, N. Jarosik, A. Kogut, M. Limon, S. S. Meyer, G. S. Tucker, E. Wollack, and E. L. Wright, “Nine-year Wilkinson Microwave Anisotropy Probe (WMAP) Observations: Cosmological Parameter Results,” *Astrophys.J.Sup* **208** (Oct., 2013) 19, [arXiv:1212.5226](#).
- [2] C. L. Bennett, D. Larson, J. L. Weiland, N. Jarosik, G. Hinshaw, N. Odegard, K. M. Smith, R. S. Hill, B. Gold, M. Halpern, E. Komatsu, M. R. Nolta, L. Page, D. N. Spergel, E. Wollack, J. Dunkley, A. Kogut, M. Limon, S. S. Meyer, G. S. Tucker, and E. L. Wright, “Nine-year Wilkinson Microwave Anisotropy Probe (WMAP) Observations: Final Maps and Results,” *Astrophys.J.Sup.* **208** (Oct., 2013) 20, [arXiv:1212.5225](#).
- [3] **Planck** Collaboration, P. A. R. Ade *et al.*, “Planck 2015 results. XIII. Cosmological parameters,” [arXiv:1502.01589](#) [[astro-ph.CO](#)].
- [4] e. a. Anderson L., “The clustering of galaxies in the SDSS-III Baryon Oscillation Spectroscopic Survey: baryon acoustic oscillations in the Data Releases 10 and 11 Galaxy samples,” *Mon. Not. Roy. Astron. Soc.* **441** (June, 2014) 24–62, [arXiv:1312.4877](#).
- [5] A. J. Cuesta, M. Vargas-Magaña, F. Beutler, A. S. Bolton, J. R. Brownstein, D. J. Eisenstein, H. Gil-Marín, S. Ho, C. K. McBride, C. Maraston, N. Padmanabhan, W. J. Percival, B. A. Reid, A. J. Ross, N. P. Ross, A. G. Sánchez, D. J. Schlegel, D. P. Schneider, D. Thomas, J. Tinker, R. Tojeiro, L. Verde, and M. White, “The clustering of galaxies in the SDSS-III Baryon Oscillation Spectroscopic Survey: baryon acoustic oscillations in the correlation function of LOWZ and CMASS galaxies in Data Release 12,” *Mon. Not. Roy. Astron. Soc.* **457** (Apr., 2016) 1770–1785, [arXiv:1509.06371](#).
- [6] A. J. Cuesta, L. Verde, A. Riess, and R. Jimenez, “Calibrating the cosmic distance scale ladder: the role of the sound horizon scale and the local expansion rate as distance anchors,” *Mon. Not. Roy. Astron. Soc.* **448** no. 4, (2015) 3463–3471, [arXiv:1411.1094](#) [[astro-ph.CO](#)].
- [7] É. e. a. Aubourg, “Cosmological implications of baryon acoustic oscillation measurements,” *Phys. Rev. D* **92** no. 12, (Dec., 2015) 123516, [arXiv:1411.1074](#).
- [8] A. G. Riess, L. Macri, S. Casertano, H. Lampeitl, H. C. Ferguson, A. V. Filippenko, S. W. Jha, W. Li, and R. Chornock, “A 3% Solution: Determination of the Hubble Constant with the Hubble Space Telescope and Wide Field Camera 3,” *Astrophys. J.* **730** (2011) 119, [arXiv:1103.2976](#) [[astro-ph.CO](#)]. [Erratum: *Astrophys. J.* 732,129(2011)].
- [9] V. Marra, L. Amendola, I. Sawicki, and W. Valkenburg, “Cosmic Variance and the Measurement of the Local Hubble Parameter,” *Physical Review Letters* **110** no. 24, (June, 2013) 241305, [arXiv:1303.3121](#) [[astro-ph.CO](#)].
- [10] L. Verde, P. Protopapas, and R. Jimenez, “Planck and the local Universe: Quantifying the tension,” *Physics of the Dark Universe* **2** (Sept., 2013) 166–175, [arXiv:1306.6766](#) [[astro-ph.CO](#)].
- [11] C. L. Bennett, D. Larson, J. L. Weiland, and G. Hinshaw, “The 1% Concordance Hubble Constant,” *Astrophys. J.* **794** (Oct., 2014) 135, [arXiv:1406.1718](#).
- [12] Planck Collaboration, P. A. R. Ade, N. Aghanim, C. Armitage-Caplan, M. Arnaud, M. Ashdown, F. Atrio-Barandela, J. Aumont, C. Baccigalupi, A. J. Banday, and et al., “Planck 2013 results. XVI. Cosmological parameters,” *Astron. Astrophys.* **571** (Nov., 2014) A16, [arXiv:1303.5076](#).
- [13] G. Efstathiou, “H₀ revisited,” *Mon. Not. Roy. Astron. Soc.* **440** (May, 2014) 1138–1152, [arXiv:1311.3461](#).
- [14] E. M. L. Humphreys, M. J. Reid, J. M. Moran, L. J. Greenhill, and A. L. Argon, “Toward a New Geometric Distance to the Active Galaxy NGC 4258. III. Final Results and the Hubble Constant,” *Astrophys. J.* **775** (Sept., 2013) 13, [arXiv:1307.6031](#).
- [15] M. Wyman, D. H. Rudd, R. A. Vanderveld, and W. Hu, “Neutrinos Help Reconcile Planck

- Measurements with the Local Universe,” *Physical Review Letters* **112** no. 5, (Feb., 2014) 051302, [arXiv:1307.7715 \[astro-ph.CO\]](#).
- [16] C. Dvorkin, M. Wyman, D. H. Rudd, and W. Hu, “Neutrinos help reconcile Planck measurements with both the early and local Universe,” *Phys. Rev. D* **90** no. 8, (Oct., 2014) 083503, [arXiv:1403.8049](#).
 - [17] B. Leistedt, H. V. Peiris, and L. Verde, “No New Cosmological Concordance with Massive Sterile Neutrinos,” *Physical Review Letters* **113** no. 4, (July, 2014) 041301, [arXiv:1404.5950](#).
 - [18] É. e. a. Aubourg, “Cosmological implications of baryon acoustic oscillation measurements,” *Phys. Rev. D* **92** no. 12, (Dec., 2015) 123516, [arXiv:1411.1074](#).
 - [19] Planck Collaboration, P. A. R. Ade, N. Aghanim, M. Arnaud, M. Ashdown, J. Aumont, C. Baccigalupi, A. J. Banday, R. B. Barreiro, N. Bartolo, and et al., “Planck 2015 results. XIV. Dark energy and modified gravity,” *ArXiv e-prints* (Feb., 2015) , [arXiv:1502.01590](#).
 - [20] A. G. Riess, L. M. Macri, S. L. Hoffmann, D. Scolnic, S. Casertano, A. V. Filippenko, B. E. Tucker, M. J. Reid, D. O. Jones, J. M. Silverman, R. Chornock, P. Challis, W. Yuan, and R. J. Foley, “A 2.4% Determination of the Local Value of the Hubble Constant,” *ArXiv e-prints* (Apr., 2016) , [arXiv:1604.01424](#).
 - [21] S. H. Suyu and et al., “H0LiCOW I. H0 Lenses in COSMOGRAIL’s Wellspring: Program Overview,” *ArXiv e-prints* (June, 2016) , [arXiv:1607.00017](#).
 - [22] V. Bonvin and et al., “H0LiCOW V. New COSMOGRAIL time delays of HE0435-1223: H_0 to 3.8% precision from strong lensing in a flat Λ CDM model,” [arXiv:1607.01790v1](#).
 - [23] G. E. Addison, Y. Huang, D. J. Watts, C. L. Bennett, M. Halpern, G. Hinshaw, and J. L. Weiland, “Quantifying Discordance in the 2015 Planck CMB Spectrum,” *Astrophys. J.* **818** (Feb., 2016) 132, [arXiv:1511.00055](#).
 - [24] D. J. Eisenstein and W. Hu, “Baryonic Features in the Matter Transfer Function,” *Astrophys. J.* **496** (Mar., 1998) 605–614, [astro-ph/9709112](#).
 - [25] J. Hamann, S. Hannestad, J. Lesgourgues, C. Rampf, and Y. Y. Y. Wong, “Cosmological parameters from large scale structure - geometric versus shape information,” *JCAP* **7** (July, 2010) 022, [arXiv:1003.3999](#).
 - [26] R. Jimenez and A. Loeb, “Constraining Cosmological Parameters Based on Relative Galaxy Ages,” *Astrophys. J.* **573** (July, 2002) 37–42, [astro-ph/0106145](#).
 - [27] A. Heavens, R. Jimenez, and L. Verde, “Standard rulers, candles, and clocks from the low-redshift Universe,” *Phys. Rev. Lett.* **113** no. 24, (2014) 241302, [arXiv:1409.6217 \[astro-ph.CO\]](#).
 - [28] L. Verde, J. L. Bernal, A. Heavens, and R. Jimenez, “The length of the local standard ruler,” [In prep.](#)
 - [29] Planck Collaboration, N. Aghanim, M. Arnaud, M. Ashdown, J. Aumont, C. Baccigalupi, A. J. Banday, R. B. Barreiro, J. G. Bartlett, N. Bartolo, and et al., “Planck 2015 results. XI. CMB power spectra, likelihoods, and robustness of parameters,” *ArXiv e-prints* (July, 2015) , [arXiv:1507.02704](#).
 - [30] F. Beutler, C. Blake, M. Colless, D. H. Jones, L. Staveley-Smith, L. Campbell, Q. Parker, W. Saunders, and F. Watson, “The 6dF Galaxy Survey: baryon acoustic oscillations and the local Hubble constant,” *Mon. Not. Roy. Astron. Soc.* **416** (Oct., 2011) 3017–3032, [arXiv:1106.3366](#).
 - [31] A. J. Ross, L. Samushia, C. Howlett, W. J. Percival, A. Burden, and M. Manera, “The clustering of the SDSS DR7 main Galaxy sample - I. A 4 per cent distance measure at $z = 0.15$,” *Mon. Not. Roy. Astron. Soc.* **449** (May, 2015) 835–847, [arXiv:1409.3242](#).
 - [32] E. A. Kazin, J. Koda, C. Blake, N. Padmanabhan, S. Brough, M. Colless, C. Contreras, W. Couch, S. Croom, D. J. Croton, T. M. Davis, M. J. Drinkwater, K. Forster, D. Gilbank, M. Gladders, K. Glazebrook, B. Jelliffe, R. J. Jurek, I.-h. Li, B. Madore, D. C. Martin, K. Pimbblet, G. B. Poole, M. Pracy, R. Sharp, E. Wisnioski, D. Woods, T. K. Wyder, and H. K. C. Yee, “The WiggleZ Dark Energy Survey: improved distance measurements to $z = 1$ with reconstruction of the baryonic acoustic feature,” *Mon. Not. Roy. Astron. Soc.* **441** (July, 2014) 3524–3542, [arXiv:1401.0358](#).
 - [33] E. Bellini and et al., “in preparation,”.
 - [34] F. Beutler, C. Blake, J. Koda, F. A. Marín, H.-J. Seo, A. J. Cuesta, and D. P. Schneider, “The

- BOSS-WiggleZ overlap region - I. Baryon acoustic oscillations,” *Mon. Not. Roy. Astron. Soc.* **455** (Jan., 2016) 3230–3248, [arXiv:1506.03900](#).
- [35] M. Betoule *et al.*, “Improved cosmological constraints from a joint analysis of the SDSS-II and SNLS supernova samples,” *Astron. Astrophys.* **568** (Aug., 2014) A22, [arXiv:1401.4064](#).
- [36] J. Lesgourgues, “The Cosmic Linear Anisotropy Solving System (CLASS) I: Overview,” [arXiv:1104.2932 \[astro-ph.IM\]](#).
- [37] D. Blas, J. Lesgourgues, and T. Tram, “The Cosmic Linear Anisotropy Solving System (CLASS) II: Approximation schemes,” *JCAP* **1107** (2011) 034, [arXiv:1104.2933 \[astro-ph.CO\]](#).
- [38] B. Audren, J. Lesgourgues, K. Benabed, and S. Prunet, “Conservative constraints on early cosmology with MONTE PYTHON,” *JCAP* **2** (Feb., 2013) 1, [arXiv:1210.7183](#).
- [39] J. Caruana, A. J. Bunker, S. M. Wilkins, E. R. Stanway, S. Lorenzoni, M. J. Jarvis, and H. Ebert, “Spectroscopy of $\bar{z} \approx 7$ candidate galaxies: using Lyman α to constrain the neutral fraction of hydrogen in the high-redshift universe,” *Mon. Not. Roy. Astron. Soc.* **443** (Oct., 2014) 2831–2842, [arXiv:1311.0057](#).
- [40] A. Gelman and D. Rubin, “Inference from iterative simulation using multiple sequences,” *Statistical Science* **7** (1992) 457–511. <http://www.stat.columbia.edu/~gelman/research/published/itsim.pdf>.
- [41] D. Foreman-Mackey, D. W. Hogg, D. Lang, and J. Goodman, “emcee: The MCMC Hammer,” *Publications of the Astronomical Society of the Pacific* **125** (Mar., 2013) 306–312, [arXiv:1202.3665 \[astro-ph.IM\]](#).
- [42] J. Goodman and J. Weare, “Ensemble samplers with affine invariance,” *Comm. App. Math. Comp.* **5** (2010) 65–80.
- [43] E. Aver, K. A. Olive, R. L. Porter, and E. D. Skillman, “The primordial helium abundance from updated emissivities,” *JCAP* **1311** (2013) 017, [arXiv:1309.0047 \[astro-ph.CO\]](#).
- [44] Y. I. Izotov, T. X. Thuan, and N. G. Guseva, “A new determination of the primordial He abundance using the He I $\lambda 10830$ Å emission line: cosmological implications,” *Mon. Not. Roy. Astron. Soc.* **445** (Nov., 2014) 778–793, [arXiv:1408.6953](#).
- [45] A. Serenelli and S. Basu, “Determining the initial helium abundance of the Sun,” *Astrophys. J.* **719** (2010) 865–872, [arXiv:1006.0244 \[astro-ph.SR\]](#).
- [46] G. Mangano, G. Miele, S. Pastor, T. Pinto, O. Pisanti, *et al.*, “Relic neutrino decoupling including flavor oscillations,” *Nucl.Phys.* **B729** (2005) 221–234, [arXiv:hep-ph/0506164 \[hep-ph\]](#).
- [47] L. Ackerman, M. R. Buckley, S. M. Carroll, and M. Kamionkowski, “Dark Matter and Dark Radiation,” *Phys.Rev.* **D79** (2009) 023519, [arXiv:0810.5126 \[hep-ph\]](#).
- [48] K. Abazajian, M. Acero, S. Agarwalla, A. Aguilar-Arevalo, C. Albright, *et al.*, “Light Sterile Neutrinos: A White Paper,” [arXiv:1204.5379 \[hep-ph\]](#).
- [49] S. Weinberg, “Goldstone Bosons as Fractional Cosmic Neutrinos,” *Phys.Rev.Lett.* **110** no. 24, (2013) 241301, [arXiv:1305.1971 \[astro-ph.CO\]](#).
- [50] C. Kelso, S. Profumo, and F. S. Queiroz, “Nonthermal WIMPs as ”Dark Radiation” in Light of ATACAMA, SPT, WMAP9 and Planck,” *Phys.Rev.* **D88** no. 2, (2013) 023511, [arXiv:1304.5243 \[hep-ph\]](#).
- [51] J. Mastache and A. de la Macorra, “Extra relativistic degrees of freedom without extra particles using Planck data,” *Phys.Rev.* **D88** (2013) 043506, [arXiv:1303.7038 \[gr-qc\]](#).
- [52] P. Di Bari, S. F. King, and A. Merle, “Dark Radiation or Warm Dark Matter from long lived particle decays in the light of Planck,” *Phys.Lett.* **B724** (2013) 77–83, [arXiv:1303.6267 \[hep-ph\]](#).
- [53] M. Archidiacono, E. Giusarma, S. Hannestad, and O. Mena, “Cosmic dark radiation and neutrinos,” *Adv.High Energy Phys.* **2013** (2013) 191047, [arXiv:1307.0637 \[astro-ph.CO\]](#).
- [54] C. Boehm, M. J. Dolan, and C. McCabe, “Increasing N_{eff} with particles in thermal equilibrium with neutrinos,” *JCAP* **1212** (2012) 027, [arXiv:1207.0497 \[astro-ph.CO\]](#).
- [55] J. Hasenkamp and J. Kersten, “Dark radiation from particle decay: cosmological constraints and

- opportunities,” *JCAP* **1308** (2013) 024, [arXiv:1212.4160 \[hep-ph\]](#).
- [56] L. A. Anchordoqui, H. Goldberg, X. Huang, and B. J. Vlcek, “Reconciling BICEP2 and Planck results with right-handed Dirac neutrinos in the fundamental representation of grand unified E_6 ,” *JCAP* **1406** (2014) 042, [arXiv:1404.1825 \[hep-ph\]](#).
 - [57] A. Solaguren-Beascoa and M. Gonzalez-Garcia, “Dark Radiation Confronting LHC in Z' Models,” *Phys.Lett.* **B719** (2013) 121–125, [arXiv:1210.6350 \[hep-ph\]](#).
 - [58] M. Gonzalez-Garcia, V. Niro, and J. Salvado, “Dark Radiation and Decaying Matter,” *JHEP* **1304** (2013) 052, [arXiv:1212.1472 \[hep-ph\]](#).
 - [59] S. Bashinsky and U. Seljak, “Neutrino perturbations in CMB anisotropy and matter clustering,” *Phys.Rev.* **D69** (2004) 083002, [arXiv:astro-ph/0310198 \[astro-ph\]](#).
 - [60] Z. Hou, R. Keisler, L. Knox, M. Millea, and C. Reichardt, “How Additional Massless Neutrinos Affect the Cosmic Microwave Background Damping Tail,” [arXiv:1104.2333 \[astro-ph.CO\]](#).
 - [61] J. Lesgourgues, G. Mangano, G. Miele, and S. Pastor, *Neutrino cosmology*. Cambridge Univ. Press, Cambridge, 2013.
 - [62] W. Hu, D. J. Eisenstein, M. Tegmark, and M. J. White, “Observationally determining the properties of dark matter,” *Phys. Rev.* **D59** (1999) 023512, [arXiv:astro-ph/9806362 \[astro-ph\]](#).
 - [63] W. Hu, “Structure formation with generalized dark matter,” *Astrophys. J.* **506** (1998) 485–494, [arXiv:astro-ph/9801234 \[astro-ph\]](#).
 - [64] R. Trotta and A. Melchiorri, “Indication for primordial anisotropies in the neutrino background from WMAP and SDSS,” *Phys.Rev.Lett.* **95** (2005) 011305, [arXiv:astro-ph/0412066 \[astro-ph\]](#).
 - [65] T. L. Smith, S. Das, and O. Zahn, “Constraints on neutrino and dark radiation interactions using cosmological observations,” *Phys.Rev.* **D85** (2012) 023001, [arXiv:1105.3246 \[astro-ph.CO\]](#).
 - [66] F.-Y. Cyr-Racine and K. Sigurdson, “Limits on Neutrino-Neutrino Scattering in the Early Universe,” [arXiv:1306.1536 \[astro-ph.CO\]](#).
 - [67] I. M. Oldengott, C. Rampf, and Y. Y. Y. Wong, “Boltzmann hierarchy for interacting neutrinos I: formalism,” [arXiv:1409.1577 \[astro-ph.CO\]](#).
 - [68] B. Audren *et al.*, “Robustness of cosmic neutrino background detection in the cosmic microwave background,” *JCAP* **1503** (2015) 036, [arXiv:1412.5948 \[astro-ph.CO\]](#).
 - [69] M. Vonlanthen, S. Rasanen, and R. Durrer, “Model-independent cosmological constraints from the CMB,” *JCAP* **1008** (2010) 023, [arXiv:1003.0810 \[astro-ph.CO\]](#).
 - [70] B. Audren, “Separate Constraints on Early and Late Cosmology,” *Mon. Not. Roy. Astron. Soc.* **444** no. 1, (2014) 827–832, [arXiv:1312.5696 \[astro-ph.CO\]](#).
 - [71] B. Audren, J. Lesgourgues, K. Benabed, and S. Prunet, “Conservative Constraints on Early Cosmology: an illustration of the Monte Python cosmological parameter inference code,” *JCAP* **1302** (2013) 001, [arXiv:1210.7183 \[astro-ph.CO\]](#).
 - [72] R. E. Angulo, S. D. M. White, V. Springel, and B. Henriques, “Galaxy formation on the largest scales: the impact of astrophysics on the baryonic acoustic oscillation peak,” *Mon. Not. Roy. Astron. Soc.* **442** (Aug., 2014) 2131–2144, [arXiv:1311.7100](#).
 - [73] Y. Rasera, P.-S. Corasaniti, J.-M. Alimi, V. Bouillot, V. Reverdy, and I. Balmès, “Cosmic-variance limited Baryon Acoustic Oscillations from the DEUS-FUR Λ CDM simulation,” *Mon. Not. Roy. Astron. Soc.* **440** (May, 2014) 1420–1434, [arXiv:1311.5662](#).
 - [74] D. Tseliakhovich and C. Hirata, “Relative velocity of dark matter and baryonic fluids and the formation of the first structures,” *Phys. Rev. D.* **82** no. 8, (Oct., 2010) 083520, [arXiv:1005.2416](#).
 - [75] N. Dalal, U.-L. Pen, and U. Seljak, “Large-scale BAO signatures of the smallest galaxies,” *JCAP* **11** (Nov., 2010) 007, [arXiv:1009.4704 \[astro-ph.CO\]](#).
 - [76] Z. Slepian and D. J. Eisenstein, “On the signature of the baryon-dark matter relative velocity in the two- and three-point galaxy correlation functions,” *Mon. Not. Roy. Astron. Soc.* **448** (Mar., 2015) 9–26, [arXiv:1411.4052](#).

- [77] N. Padmanabhan and M. White, “Calibrating the baryon oscillation ruler for matter and halos,” *Phys. Rev. D* **80** (Sep, 2009) 063508. <http://link.aps.org/doi/10.1103/PhysRevD.80.063508>.
- [78] J. A. Blazek, J. E. McEwen, and C. M. Hirata, “Streaming Velocities and the Baryon Acoustic Oscillation Scale,” *Phys. Rev. Lett.* **116** (Mar, 2016) 121303. <http://link.aps.org/doi/10.1103/PhysRevLett.116.121303>.
- [79] Z. Slepian *et al.* . (in preparation) .